DESIGN FOR TORSION IN BEAM

Lokesh Lonare

ABSTRACT :
This paper investigates the torsional load capacities of two reinforced concrete cap beams in the elevated guideway structures. One beam has a regular configuration and the other has an irregular configuration. For each beam type, a 1/2-scale model was tested. The failure mechanisms of both beams were dominated by torsion. The load capacity of the regular beam was governed by the yielding of the main longitudinal reinforcement induced by a truss action. The capacity of the irregular beam was governed by a torsional crack through the columns zone, which can be attributed to the lack of confinement in the region. The large spacing of the top horizontal ties in the regular beam led to vertical splitting cracks when the beam was loaded through the shear keys. Nonlinear finite element analyses have been conducted on the beams. The finite element models are able to reproduce the nonlinear behaviors observed in the tests with reasonably good accuracy. Based on the experimental observations and numerical results, strut-&-tie models have been developed to evaluate the load capacities of the beams. Both types of models have indicated that the horizontal load resistance of a cap beam under bending and torsion will decrease with the decrease of the vertical load.

KEYWORDS:
Bent caps; reinforced concrete beams; finite element method; strut-&-tie model; torsion; earthquake performance

1. INTRODUCTION

This paper presents the experimental and numerical studies of the torsional load capacities of two reinforced concrete cap beams in elevated guideway structures of the Bay Area Rapid Transit (BART) system. Even though the torsional capacity of reinforced concrete (RC) members has been studied by many researchers, and different analytical methods have been proposed (Hsu 1984; Collins and Mitchell 1991), attention has been focused on prismatic members that have much simpler geometry and reinforcement details than the cap beams studied here. Similarly, the shear and torsion design provisions in the current ACI-318 (ACI 2005) and AASHTO LRFD Specifications (AASHTO 2004) are based on a simplified space truss analogy for a prismatic member. Even though more general strut-&-tie models are permitted by these codes, little guidance is available for the analysis of a cap beam under combined bending, shear, and torsion using a truly 3-D model.

To fill the current knowledge gap, two representative cap beams of the BART elevated guideway structures that were designed in the 1960's were selected for an experimental investigation (Shing et al. 2007). One was a regular cap beam design and the other was an irregular beam design. For each beam type, a 1/2-scale model was tested. In addition to the experimental study, nonlinear finite element analyses have been conducted to evaluate the strength and load-deformation behaviors of the test beams and to estimate their horizontal load capacities under different vertical loads. Based on the experimental and numerical results, simple strut-&-tie models have been developed. This paper summarizes the test specimens, testing procedures, and experimental and numerical results. Design implications derived from these studies are also discussed.

2. TEST PROGRAM

Beam Specimens

The design of the regular beam model is shown in Fig. 1. No. 4 (12.70 mm) and 5 (15.87 mm) bars were used for the main longitudinal reinforcement near the top of the beam and the stirrups were No. 3 bars and had a spacing of 2-3/4 in. (70 mm) on center. The stirrups in the beam outside the column zone were not closed at the top because the top horizontal ties had a much larger spacing than the U bars as in the as-built structure. Furthermore, the beam had spiral confinement extending from the column. The design of the irregular beam model is shown in Fig. 2. The stirrups were No. 3 (9.52 mm) bars at 3-1/2 in. (89 mm) on center. In this beam, all the stirrups were closed with top horizontal ties. The ties had 90-degree hooks. However, the beam did not

have horizontal confinement in the column zone.

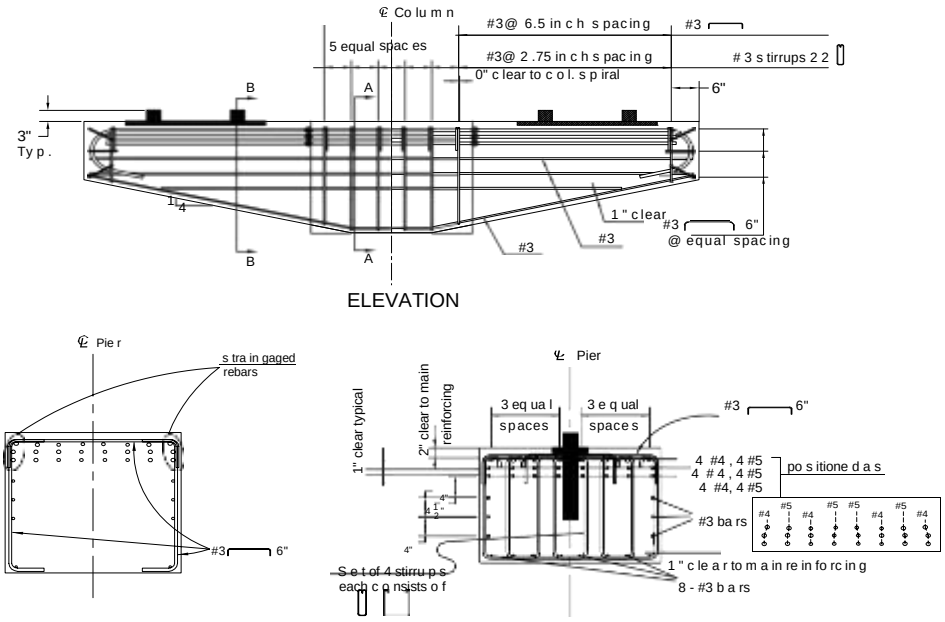

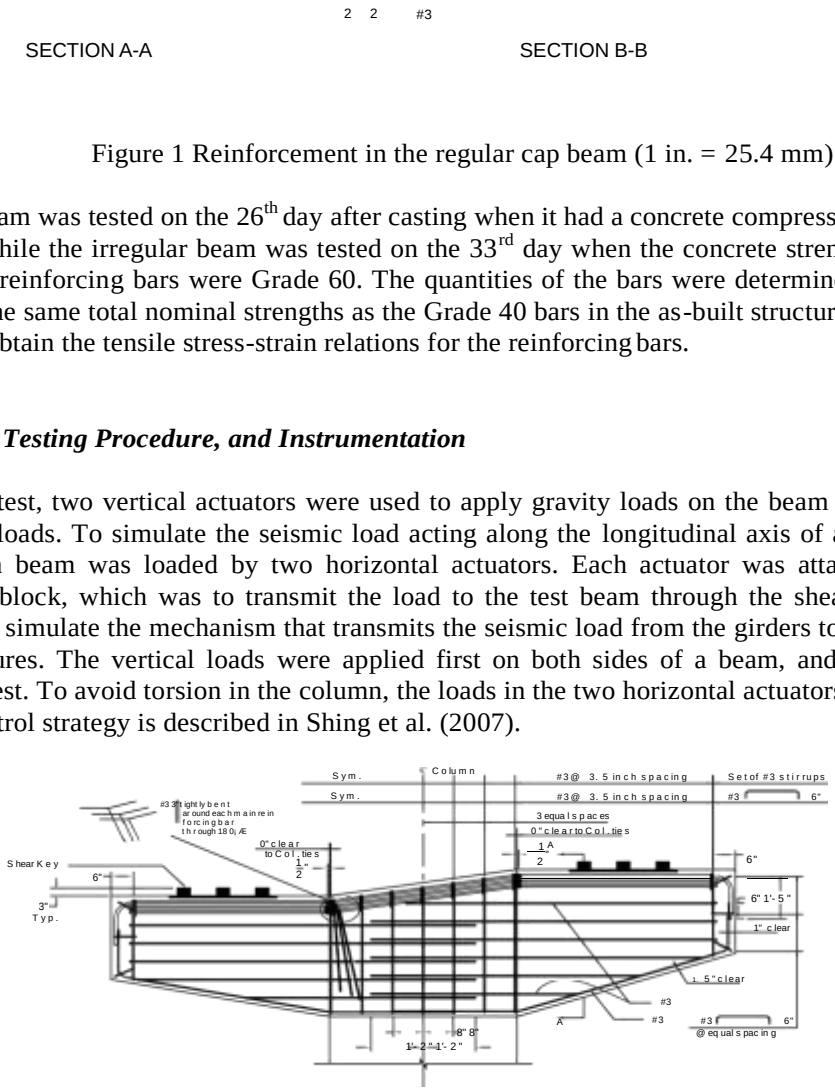

Figure 1 Reinforcement in the regular cap beam (1 in. = 25.4 mm)

The regular beam was tested on the 26th day after casting when it had a concrete compressive strength of 4.7 ksi (32.4 MPa), while the irregular beam was tested on the 33rd day when the concrete strength was 5.1 ksi (35.2 MPa). All the reinforcing bars were Grade 60. The quantities of the bars were determined in such a way that they provide the same total nominal strengths as the Grade 40 bars in the as-built structures. Tension tests were conducted to obtain the tensile stress-strain relations for the reinforcing bars.

Test Setup, Testing Procedure, and Instrumentation

In each beam test, two vertical actuators were used to apply gravity loads on the beam specimen, simulating dead and live loads. To simulate the seismic load acting along the longitudinal axis of an elevated guideway structure, each beam was loaded by two horizontal actuators. Each actuator was attached to a reinforced concrete load block, which was to transmit the load to the test beam through the shear keys. This loading scheme was to simulate the mechanism that transmits the seismic load from the girders to the cap beams in the as-built structures. The vertical loads were applied first on both sides of a beam, and maintained constant throughout a test. To avoid torsion in the column, the loads in the two horizontal actuators were maintained the same. The control strategy is described in Shing et al. (2007).

SECTION A-A

Figure 2 Reinforcement in the irregular cap beam (1 ft. = 305 mm; 1 in. = 25.4 mm)

Figure 3 shows the location of strain gages installed on the irregular beam. In addition, displacement transducers and inclinometers were used to measure the beam deflection and rotation. The same instrumentation scheme and sensor numbering were used for the regular beam. Strain gages were attached to the main longitudinal bars at locations close to the two sides of the column zone. Two gages were placed at each location on opposite sides of a bar to provide some redundancy. These gages are designated as STxA and STxB, where x is a number indicating the gage location as shown in Fig. 3.

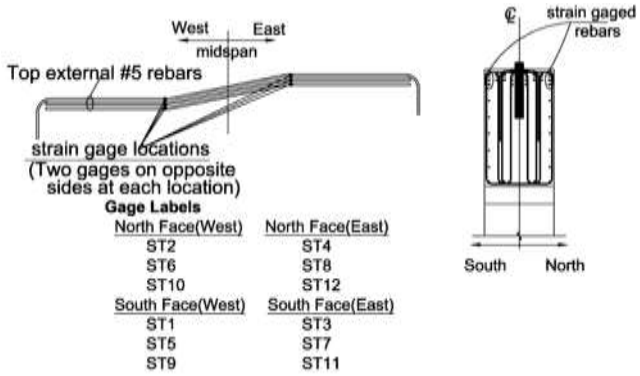

Figure 3 Strain gage locations for the irregular cap beam

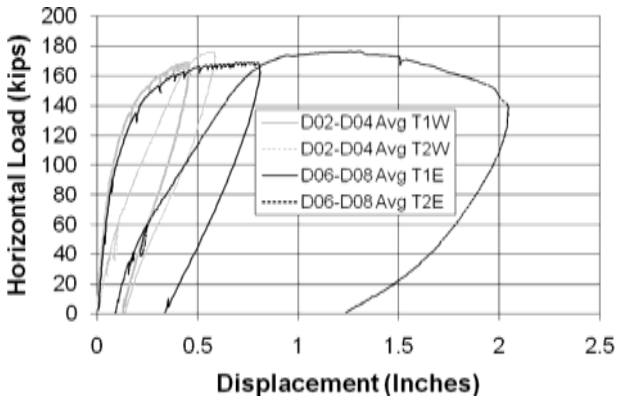

Figure 4 Horizontal load-vs.-averaged end displacement curves for the regular beam (1 in. = 25.4 mm; 1 kip = 4.45 kN)

3. TEST RESULTS

Regular Cap Beam

In testing the regular beam, a vertical load of 150 kips (668 kN) was first applied on each side of the beam and maintained constant afterwards. Two horizontal load tests (T1 and T2) were conducted on this beam. The load-averaged displacement curves are shown in Fig. 4. The averaged end displacement is calculated with the readings from one top and one bottom displacement transducers to take out the rotation of the beam. In the first test, the horizontal loads were transmitted through the shear keys. The horizontal loads were applied towards south. During this test, a vertical splitting crack occurred in the beam on the east side adjacent to the shear key, limiting the capability of the shear key to carry additional load. The test was, therefore, stopped. Neoprene pads, which were 1-1/2-in. (38-mm) thick, were then inserted in the gaps between the north face of the beam and the load blocks. The beam was then tested again by pushing against its north face through the pads.

The damage of the regular beam at the final stage is shown in Fig. 5. It can be observed that the east side of the beam had the most severe damage while the west side suffered relatively light damage. In the first test (T1), diagonal torsional shear cracks were first observed on the south face at a horizontal load of 135 kips (601 kN) per actuator, and slightly inclined flexural-torsional cracks were observed in the lower part of the north face along the two sides of the column zone. A vertical splitting crack initiated on the east side of the beam at a load of 149 kips (663 kN). This crack started from an inclined torsional crack on the top face of the beam and propagated along the north edge of the steel plate for the shear key all the way to the east end of the beam. This limited the capability of the shear key to transmit any load beyond 169 kips (752 kN).

West  East

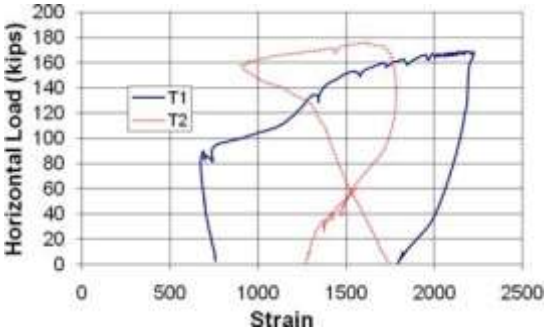

Figure 5 Damage in the regular beam

Figure 6 Horizontal load vs. bar btrain (in micro-strain) from gage ST3B in the regular beam (1 kip = 4.45 kN)

In the second test, the horizontal loads were transmitted through neoprene pads that filled the gaps between the north face of the beam and the load blocks. In this test, severe torsional cracks developed. The crack pattern in Fig. 5 shows the development of compression struts in a truss mechanism. This induced tension in the main longitudinal reinforcement as indicated by the measured strains. The maximum load reached in this test was 176 kips (783 kN). Because of the short span length of the beam, the inclined torsional cracks propagated into the column zone. Hence, the spiral confinement that extended into the column zone should have contributed to the torsional resistance of the beam.

Figure 6 shows a plot of the horizontal load vs. the strain measured by Gage ST3B, which was located on the east side close to the south face of the beam. The horizontal load acted towards south. It can be noted that the bar had an initial tensile strain of about 0.0008 in the first test (T1), which was induced by the 150-kip (668-kN) vertical load. As the horizontal load increased, the tensile strain decreased at the beginning due to bending until a horizontal load of about 80 kips (356 kN) was reached. Beyond 80 kips (356 kN), the trend was reversed and the tensile strain increased with the horizontal load due to a truss mechanism. The bar barely reached yield at 169 kips (752 kN) and the residual strain after the removal of the horizontal load was about 0.0018. In the second test (T2), the initial tensile strain was about 0.0013 and it increased with the horizontal load until a load of about 130 kips (579 kN) was reached. After this, the tensile strain started to decrease as the bending action began to dominate, probably due to the loss of the compression strut action. The decrease in tensile strain accelerated after the peak load of 176 kips (783 kN) was passed.

Irregular Cap Beam

In testing the irregular beam, a vertical load of 175 kips (779 kN) was first applied on each side of the beam. The beam was then loaded towards south passing its peak resistance with two horizontal actuators. Then, the displacement was reversed passing its peak resistance in the other direction. Finally, the beam was loaded towards south again and then unloaded.

The damage of the irregular beam induced by the horizontal displacement cycles is shown in Fig. 7. When loaded towards south, vertical cracks first developed in the column zone and some slightly inclined flexural-torsional cracks developed in the lower part of the north face, and a diagonal torsional crack developed on the south face of the west side of the beam at about 166 kips. At about 170 kips (757 kN), a more or less horizontal crack developed in the column zone on the north face right at the elevation where the vertical steel was terminated, as shown in Fig. 8. After the development of this crack, the south face of the column zone tended to rotate more than the north face as the beam was pushed further towards south. This is very likely due to the development of a vertical or inclined crack plane in the column zone separating the region into two portions. However, the load continued to increase to a peak of 180 kips (801 kN). At this point, cracks on the south face were very minor. After the peak load, the horizontal crack on the north face was joined by the flexural-torsional cracks from the bottom and some concrete spalling was observed as shown in Fig. 8.

The horizontal load-vs.-averaged horizontal end displacement curves are shown in Fig. 8. The displacement at the west end is smaller than that at the east. The load-displacement curves show that nonlinearity initiates at about 100 kips (446 kN). The loading direction was reversed towards north at the point where the horizontal resistance decreased from the peak value of 180 kips (801 kN) to about 150 kips (668 kN) as shown in Fig. 8. The maximum load reached in the other direction is about 160 kips (712 kN). A horizontal crack similar to that developed on the north face in the column zone occurred on the south face. After the peak, the load was reversed again. When the beam was loaded towards south for the second time, the maximum resistance dropped to about 104 kips (463 kN).

Figure 7 Damage in the irregular beam

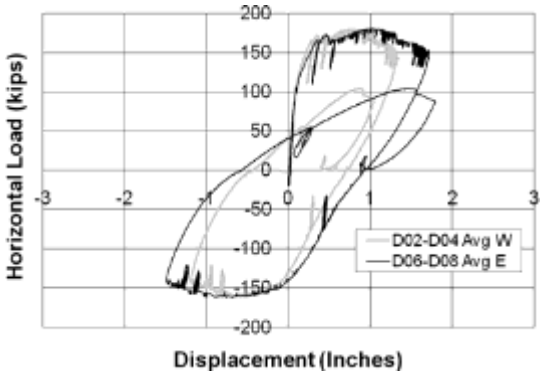

Figure 8 Horizontal Load vs. averaged end displacement curves for the irregular beam (1 in. = 25.4 mm; 1 kip = 4.45 kN)

4. NONLINEAR FINITE ELEMENT MODELING

The finite element program ABAQUS Version 6.51 (2005) has been used for the analyses reported here. Concrete is modeled with a 3-D damage-plasticity constitutive law that has been originally proposed by Lubliner et al. (1989) and later improved by Lee and Fenves (1998), while steel reinforcement is represented by an elastic-hardening plastic bar element. Twenty-node solid elements are used to model the concrete beams.

Figure 9 shows the plots of the horizontal load vs. horizontal displacement at the east end of the regular beam for both load cases. The numerical result for Load Case 1 shows a significant drop of load resistance after the peak. This is accompanied by the yielding of the top transverse ties and tensile splitting cracks occurring along the edges of the steel plates. This resembles what that is observed in the test.

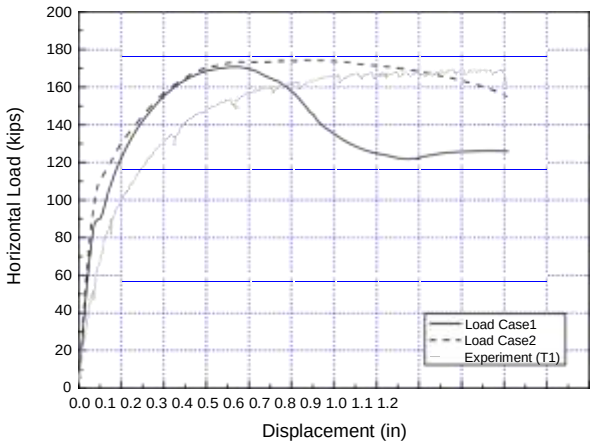

Figure 9 Horizontal load-vs.-displacement at the top of the east end of the regular beam (1 in. = 25.4 mm; 1 kip = 4.45 kN)

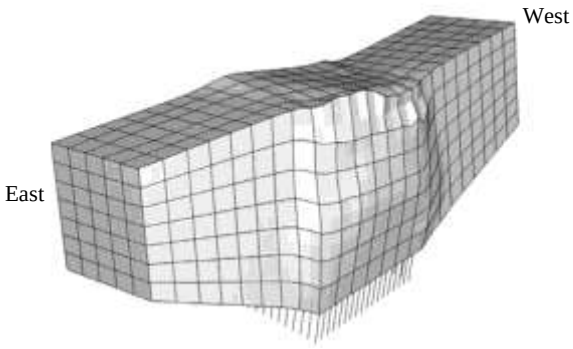

Figure 10 Deformed mesh for the irregular beam

For the irregular beam, the numerical results also match the test results reasonably well. Figure 10 shows the deformed mesh of the finite element model, which has a similar damage pattern as that observed in the test (see Fig. 7).

5. STRUT-&-TIE MODELS

Little guidelines are available in current codes (ACI 2005; AASHTO 2004) for 3-D strut-&-tie modeling of concrete members. The behaviors of the cap beams considered in this study are complicated. The beams are relatively short as compared to the cross-sectional dimensions. As a result, their capacities are significantly influenced by the torsional cracks propagating into the column zone. Hence, to develop appropriate strut-&-tie models for these beams, we have to rely on the observations from the beam tests and the results of the finite element analyses. The models proposed here are based the assumption that the load resisting mechanism of a beam is governed by the yielding of the tension ties rather than the compression failure of the diagonal struts. This assumption is consistent with the experimental observations and finite element analysis results.

The configuration of the strut-&-tie model developed for the regular beam is shown in Fig. 11. The segment of the beam starting from the free end to the centroid of the shear key on each side are ignored as the applied vertical and horizontal loads are assumed to be at the centroids of the shear keys. The tension ties are modeled with elastic-perfectly plastic truss elements. The determination of the tie areas is described in Shing et al. (2007). The yield strengths of the ties is based on the values obtained from the material tests. The cross-sectional areas of the compression struts are arbitrarily assumed to be size has negligible influence on the load capacity of the model. Under a vertical load of 150 kips (668 kN) on each side, the maximum horizontal resistance attained by the strut-&-tie model is 165 kips (734 kN), which is a little less than those obtained in the test and finite element analysis.

A similar strut-&tie model has been constructed for the irregular beam. Again, the results are on the conservative side as compared to those of the test and finite element analysis.

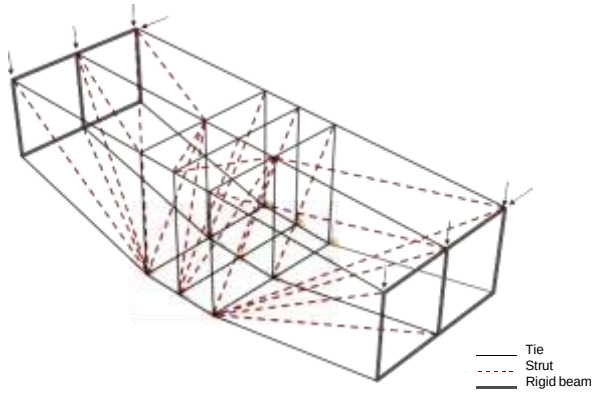

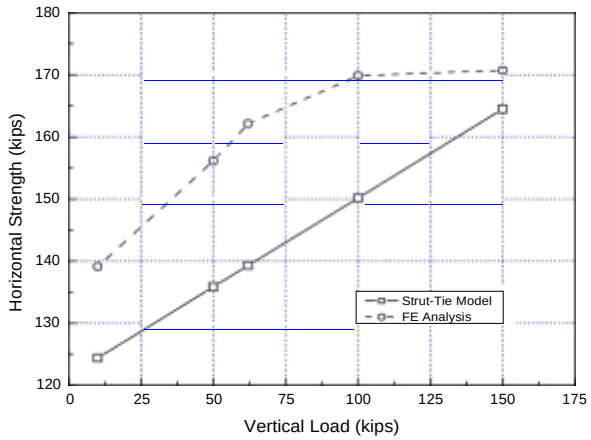

Figure 11 Strut-&-tie model for the regular beam

Figure 12 Influence of vertical load on the horizontal resistance for the regular beam (1 kip = 4.45 kN)

6. INFLUENCE OF VERTICAL LOADS

In actual structures, the vertical loads exerted on a cap beam may vary depending on the live-load condition. A study is conducted to examine the influence of the vertical load on the horizontal load capacities of the cap beams using the finite element and strut-&-tie models. The results obtained for the regular beam are shown in Fig. 12. Similar influence has been observed for the irregular beam. In both cases, the horizontal load capacities increase with the vertical load.

In the test, a 150-kip (668-kN) vertical load was applied on each side of the regular beam. This is 20% higher than the maximum expected dead and live loads. However, a cap beam could be subjected to the weight of the girders alone. The dead load due to the girders is estimated to be 62 kips (276 kN) for the ½-scale model. As shown by the finite element analysis results in Fig. 12, the horizontal load capacity of the regular beam will drop from 170 to 162 kips (757 to 721 kN) when the vertical load is reduced from 150 to 62 kips (668 to 276 kN). For the irregular beam, the dead load of the girders is estimated to be 86 kips (383 kN) while that applied in the test is 175 kips (779 kN). When the vertical load is reduced from 175 to 86 kips (779 to 383 kN), the horizontal load capacity on the west side (which is the weak side) will drop from 180 to 151 kips (801 to 672 kN) according to the finite element model. The strengths calculated with the strut-&-tie models are even lower. According to the strut-&-tie models, the horizontal load capacity of the regular beam is governed by the tensile yielding of the bottom longitudinal ties while that of the irregular beam is also influenced by the yielding of the middle vertical ties adjacent to the column zone. In either situation, the vertical loads tend to lower the force demands in these ties, and thereby, increase the horizontal load capacities.

7. CONCLUSIONS

The behaviors of the two beam specimens underscore the complexity of the load resisting mechanisms of a cap beam under simultaneous bending, shear, and torsion. The test results have shown that in addition to the stirrups, the longitudinal reinforcement and the presence or absence of confinement in the column zone play a major role in the torsional resistance of a cap beam. This load resisting mechanism cannot be properly represented by the simple space truss analogy that has been assumed in the ACI design formulas.

The finite element models developed here are able to reproduce the nonlinear behaviors of the cap beams observed in the tests with reasonably good accuracy. The models accurately capture the different failure modes of the regular and irregular beams. The strengths obtained from the analyses match the test results well. However, the finite element models show a stiffer post-crack response and a more pronounced load drop after the peak loads.

Results obtained with the strut-&-tie models are more conservative than those of the finite element analyses. Because of the simplicity, the strut-&-tie analyses have provided a good understanding of the load resisting mechanisms of the regular and irregular beams and the influence of the vertical load on the horizontal load capacities. The column zone failure observed in the irregular beam can be attributed to the higher quantity of the top longitudinal reinforcement, the lack of confinement in the column, and the deeper beam section.

Both the finite element and strut-&-tie models have indicated that the horizontal load capacity of a cap beam will decrease with the decrease of the vertical load. This has to be taken into consideration in the evaluation of actual bent caps. It is desirable that additional tests be conducted on similar cap beams under different vertical loads so that more data are available to evaluate the models proposed here.

ACKNOWLEDGMENTS

The study presented here was funded by BART through Bechtel Corporation. The input of the Bechtel/HNTB

team involved in the seismic retrofit project is gratefully acknowledged. The authors also appreciate the technical assistance of Dr. Christopher Latham and other staff members of the Powell Laboratories in the experimental work. Visiting researcher Carlo Piotti supervised the construction of the specimens, and undergraduate students Kristen Ward and Jeffrey McMaster assisted in the beam tests and data analysis. The participation of the latter was made possible by the REU Summer Internship Program of PEER. However, the opinions expressed in this paper are those of the writers and do not necessarily reflect those of the sponsor.

REFERENCES

AASHTO (2004). AASHTO LRFD Bridge Design Specifications. American Association of State Highway and Transportation Officials, 3rd ed.

ABAQUS Manual (2005): Example Problems, Verification, Theory. Version 6.51, Hibbit, Karlsson and Sorenson, Inc.

ACI-318 (2005). Building Code Requirements for Reinforced Concrete. American Concrete Institute, Farmington Hills, MI.

Collins, M.P. and Mitchell, D. (1991). Prestressed Concrete Structures, Prentice Hall, NJ.

Hsu, T.T.C. (1984). Torsion of Reinforced Concrete, Van Nostrand Reinhold, NY.

Lee, J. and Fenves, G. L. (1998). Plastic-damage model for cyclic loading of concrete structures. *Journal of Engineering Mechanics* **124:8**, 892–900.